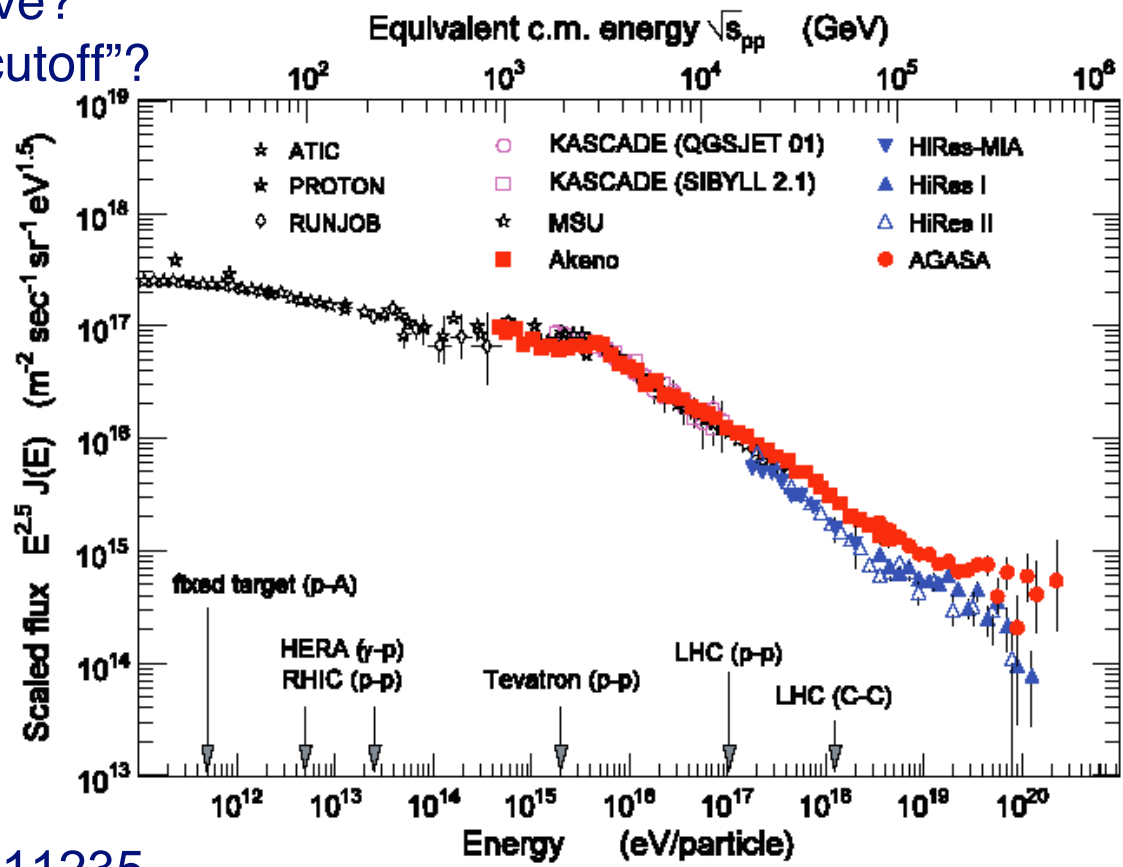


The ankle: the EHE region

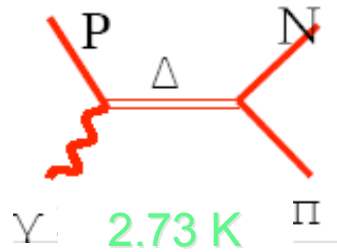
Ankle: $E^{-2.7}$ at $E \sim 10^{19}$ eV could suggest a new light population Protons are favored by all experiments.
favored by all experiments.

- What is the acceleration mechanism at these energies?
- Which are the sources? Are there extra-galactic components?
- Which particles do we observe?
- Is there the expected GZK “cutoff”?



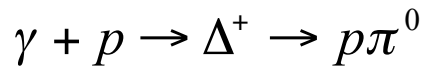
<http://arxiv.org/pdf/astro-ph/0511235>

Threshold for GZK cut-off [Greisen 66; Zatsepin & Kuzmin66]

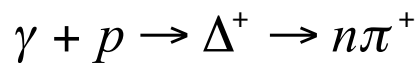


Threshold for $p-\gamma \rightarrow \Delta \rightarrow \pi N$

$$E_{k,p} = \frac{\left(\sum_f M_f\right)^2 - (m_t + m_p)^2}{2m_t} = \frac{(m_N + m_\pi)^2 - m_p^2}{2m_p}$$



$$E_\gamma = 145 \text{ MeV}$$



$$E_\gamma = 150 \text{ MeV}$$

in frame where p is at rest

Energy of CMB photons: $= 3k_B T$ effective energy for Planck spectrum

$$\varepsilon_\gamma = 3 [2.73] 8.62 \cdot 10^{-5} \text{ eV}$$

And their energy in the proton rest frame is

$$E_\gamma = \gamma_p \varepsilon_\gamma = 150 \text{ MeV}$$

$\Rightarrow \gamma_p = 2 \cdot 10^{11}$ and the threshold energy of the proton is then

$$E_p = \gamma_p m_p = 2 \cdot 10^{20} \text{ eV}$$

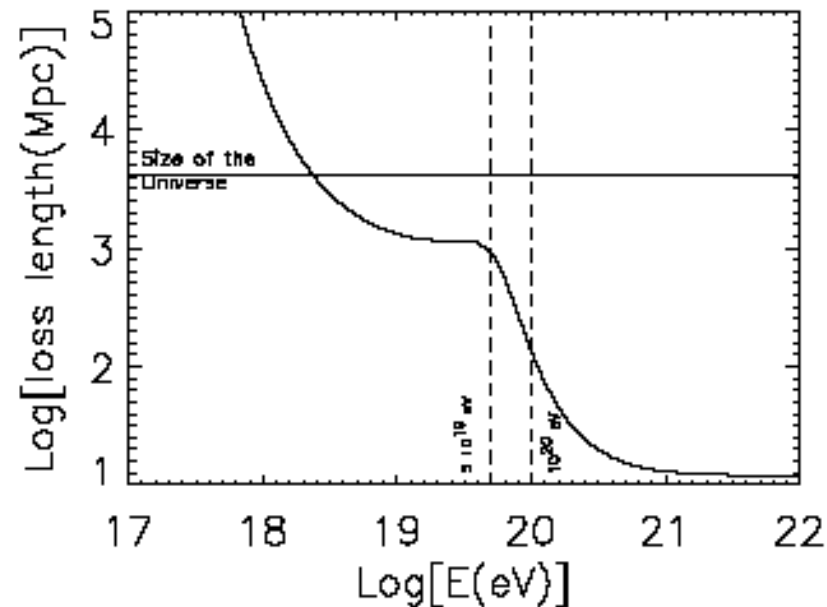
Integrating over Planck spectrum $E_{p,\text{th}} \sim 5 \cdot 10^{19} \text{ eV}$

The ankle: the EHE region

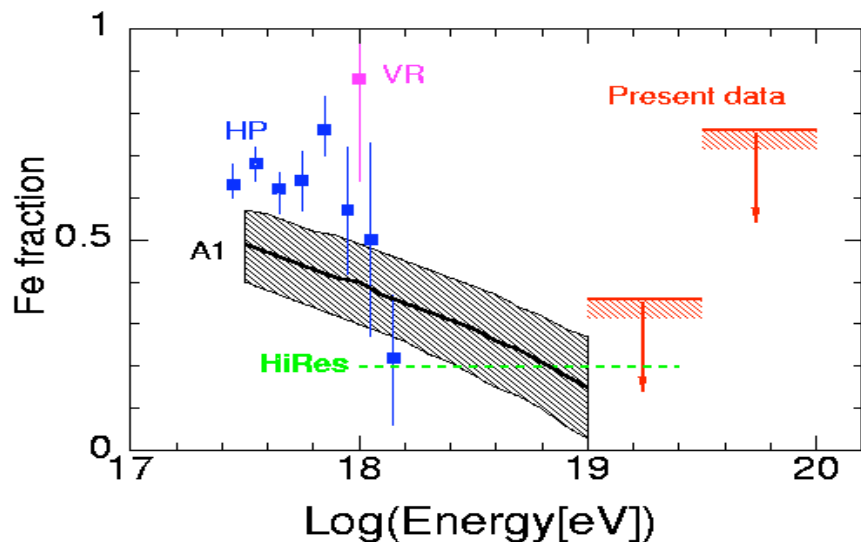
The loss length due to pair production and photopion production is about 100 Mpc at 10^{20} eV, at $2 \cdot 10^{18}$ eV the loss length due to pair production equals the dimension of the universe $p + \gamma \rightarrow \pi + \text{anything}$

The spectrum is expected to drop above the photopion production threshold

Prof. Eli Waxman lecture



Spectrum and composition in the ankle region



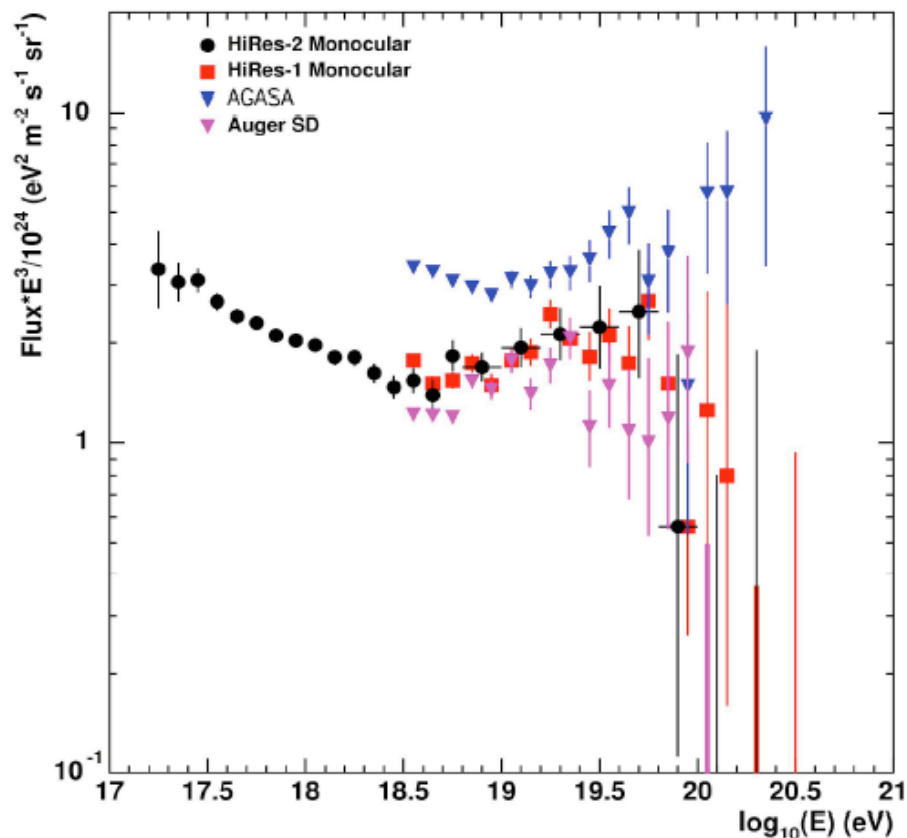
AGASA

Fe frac. (@90% CL): $< 35\%$ ($10^{19} - 10^{19.5}$ eV),
 $< 76\%$ ($E > 10^{19.5}$ eV)

Gamma-ray fraction upper limits (@90%CL)

34% ($> 10^{19}$ eV) ($\gamma/p < 0.45$)

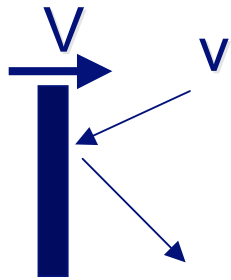
56% ($> 10^{19.5}$ eV) ($\gamma/p < 1.27$)



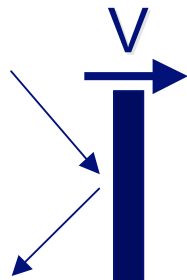
2nd order Fermi acceleration (1st version 1949)

Magnetic clouds in interstellar medium moving at velocity V (that remains unchanged after the collision with a relativistic particle $v \sim c$)

The probability of head-on encounters is slightly greater than following collisions

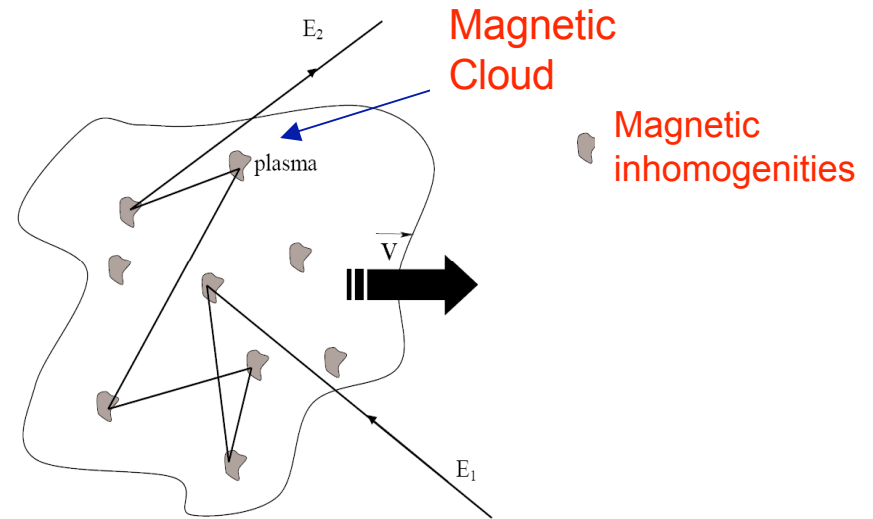


Head-on
particle gains
momentum



Overtaking
particle loses
momentum

Rate of collisions: $v_+ = \frac{v+V}{L}$ $v_- = \frac{v-V}{L}$



$$\Delta p = 2m\gamma V$$

$$\Delta p = -2m\gamma V$$

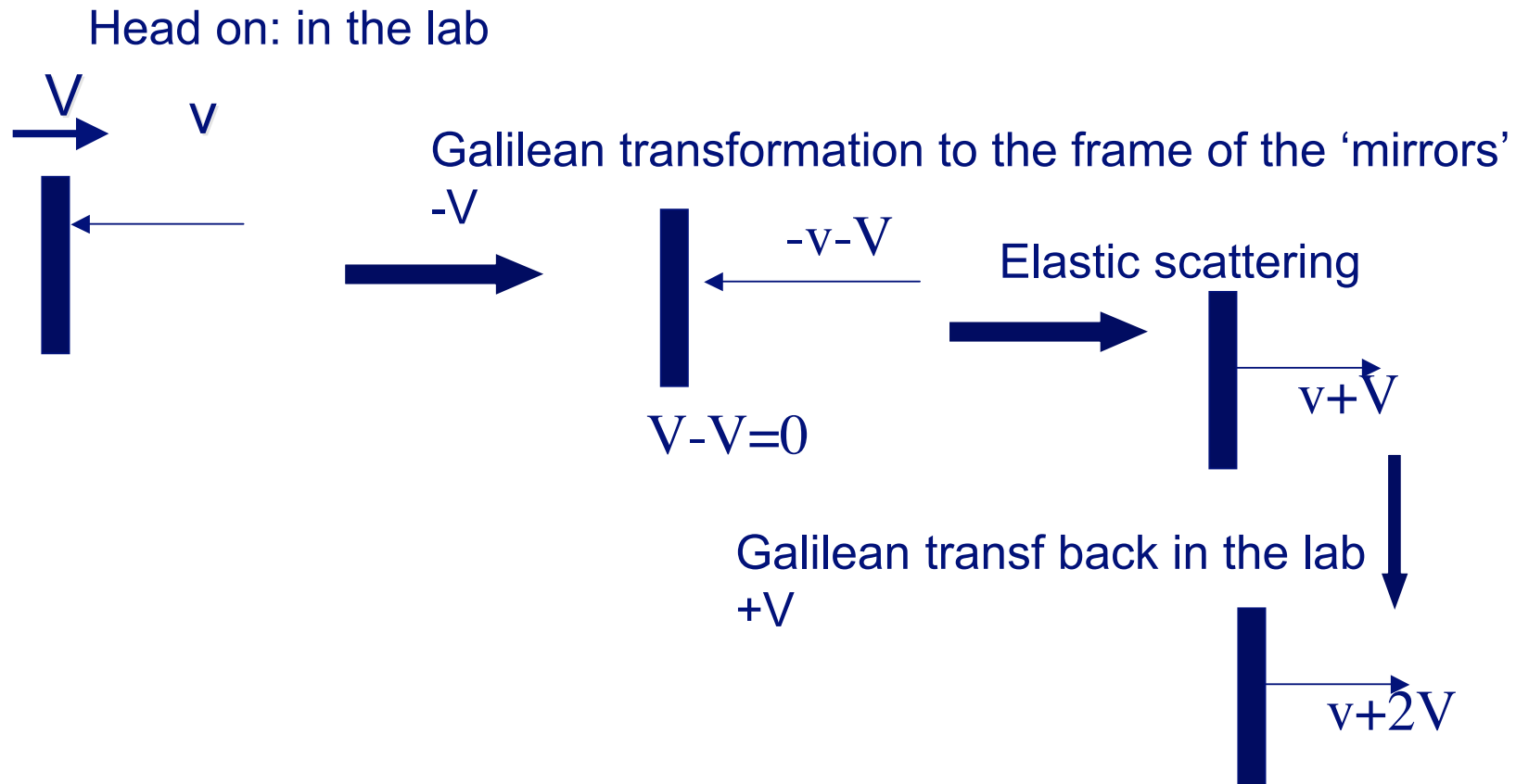
$$\Delta E = \Delta p v$$

This results in a net energy gain per collision of

$$\begin{aligned} \frac{dE}{dt} &= v_+ v \Delta p - v_- v \Delta p = \left(\frac{2V}{L} \right) 2m\gamma v V = \\ &= 4 \frac{V^2}{L} m\gamma v = \frac{E}{c} 4 \frac{V^2}{L} \end{aligned}$$

2nd order in the
velocity of the cloud

Why?



$$\Delta p = m\gamma(v+2V-v)$$

1st order Fermi acceleration (Longair vol 2)

The 2nd order mechanism is a slow process.
The 1st order is more efficient since only head-on collisions in shock waves

A shock is a transition layer where the velocity field of the fluid suddenly decreases

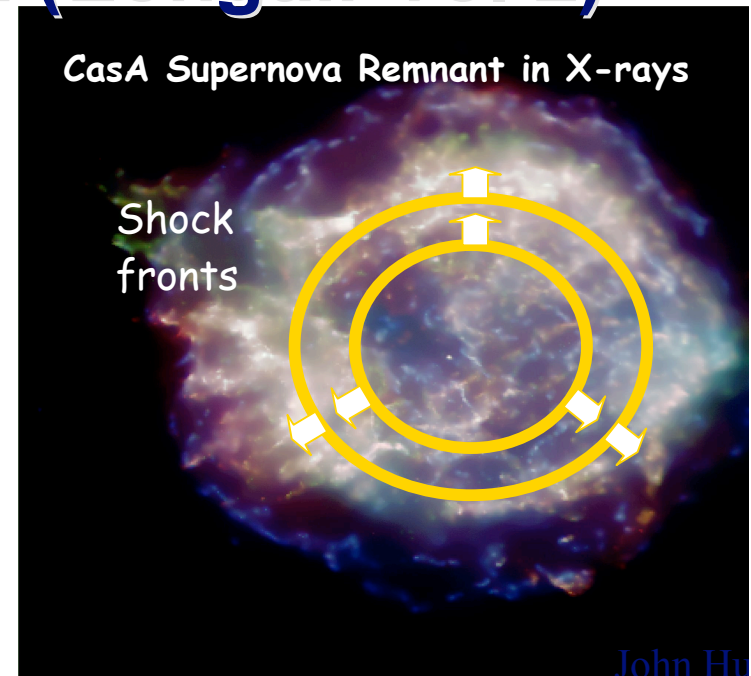
For a strong shock the shock wave moves at a highly supersonic velocity U .

In the shock rest frame: the upstream gas flows into the shock front at velocity $v_1 = U$ and leaves the shock with downstream velocity v_2 . Equation of Continuity (cons. of mass across the front):

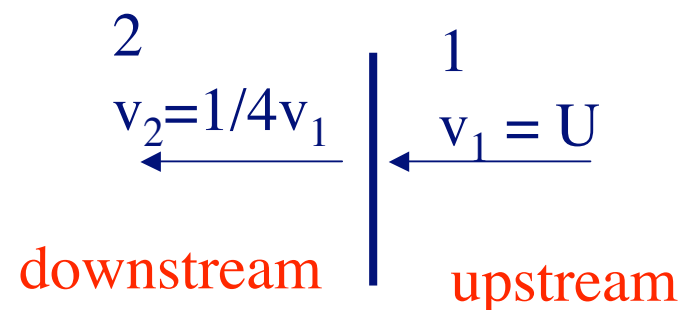
$$v_1 \rho_1 = v_2 \rho_2$$

For ionized gas $R =$ compression ratio $= \rho_2 / \rho_1 = 4$

$$\Rightarrow v_2 = 1/4 v_s < v_1 = U$$



1nd order in the velocity of the shock

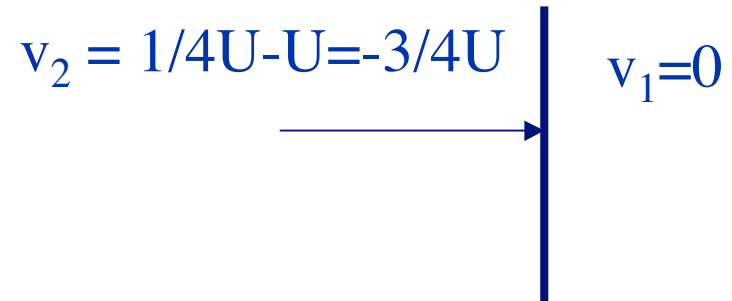


1st order Fermi acceleration (Longair vol 2)

Let's consider the particles ahead of the shock (**upstream**). Here the particle distribution is isotropic. The shock advances through the medium at velocity U , but the gas behind the shock travels at velocity $3/4U$ relative to the upstream gas.

When a high energy particle crosses the shock front, it obtains a small increase in the energy of the order of $\Delta E/E \sim U/c$

1nd order in the velocity of the shock

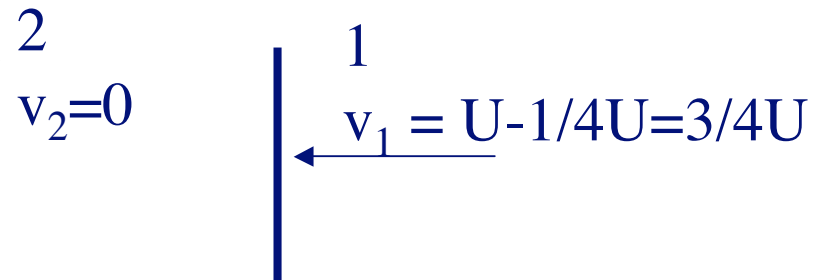


Let us consider the opposite process of a particle diffusing from behind the shock (**downstream**) to the upstream region. The velocity distribution of particles is isotropic downstream the shock and when they cross the shock front they encounter gas moving towards the shock front with the velocity $3/4U$.

The particle undergoes exactly the same process of receiving a small increase in the energy on crossing the shock from downstream to

Upstream. **So every time the particle crosses the shock it receives an increase of energy**

(more efficient!!) and the increment is the same in both directions



Fermi mechanism and power laws

$E = \beta E_0$ = average energy increase of particle after 1 round trip

$\beta = E/E_0 = 1 + U/c$ for $U \ll c \Rightarrow \ln \beta = \ln(1 + U/c) \sim U/c$

Average number of particles crossing the shock in both directions $1/4 Nc$

with N = number density of particles. Rate of losses across the shock $1/4 NU$

So the fraction of particles lost is $(1/4 NU)/(1/4 Nc) = U/c$

P = probability of crossing shock again or that particle remains in acceleration region after a collision = $1 - U/c$

And $\ln(1 + P) = \ln(1 + U/c) \sim U/c$ if $U \ll c$ so that $\ln P / \ln \beta \sim -1$

After k collisions: $E = \beta^k E_0$ and $N = N_0 P^k$ = number of particles

$$\left. \begin{array}{l} \frac{E}{E_0} = \beta^k \Rightarrow k \ln \beta = \ln \frac{E}{E_0} \\ \frac{N}{N_0} = P^k \Rightarrow k \ln P = \ln \frac{N}{N_0} \end{array} \right\} \Rightarrow k = \frac{\ln \frac{E}{E_0}}{\ln \beta} = \frac{\ln \frac{N}{N_0}}{\ln P} \Rightarrow$$

$$\ln \frac{N}{N_0} = \frac{\ln P}{\ln \beta} \times \ln \frac{E}{E_0} = \ln \left(\frac{E}{E_0} \right)^{\ln P / \ln \beta} \Rightarrow \frac{N}{N_0} = \left(\frac{E}{E_0} \right)^{\ln P / \ln \beta}$$

$$\text{differentiating } dN \propto E^{\ln P / \ln \beta - 1} dE \Rightarrow \frac{dN}{dE} \propto E^{-2}$$

CR acceleration at sources: Bottom-up

$$E_{\max} \approx \Gamma Z \left(\frac{B}{1\mu\text{G}} \right) \left(\frac{R}{1\text{kpc}} \right) 10^{18} \text{ eV}$$

Hillas Plot

SN provide right power for galactic CRs up to the knee:

CR energy density:

$$\rho_E \sim 1 \text{ eV/cm}^3 \sim B_{\text{galactic}}^2 / 8\pi$$

Needed power:

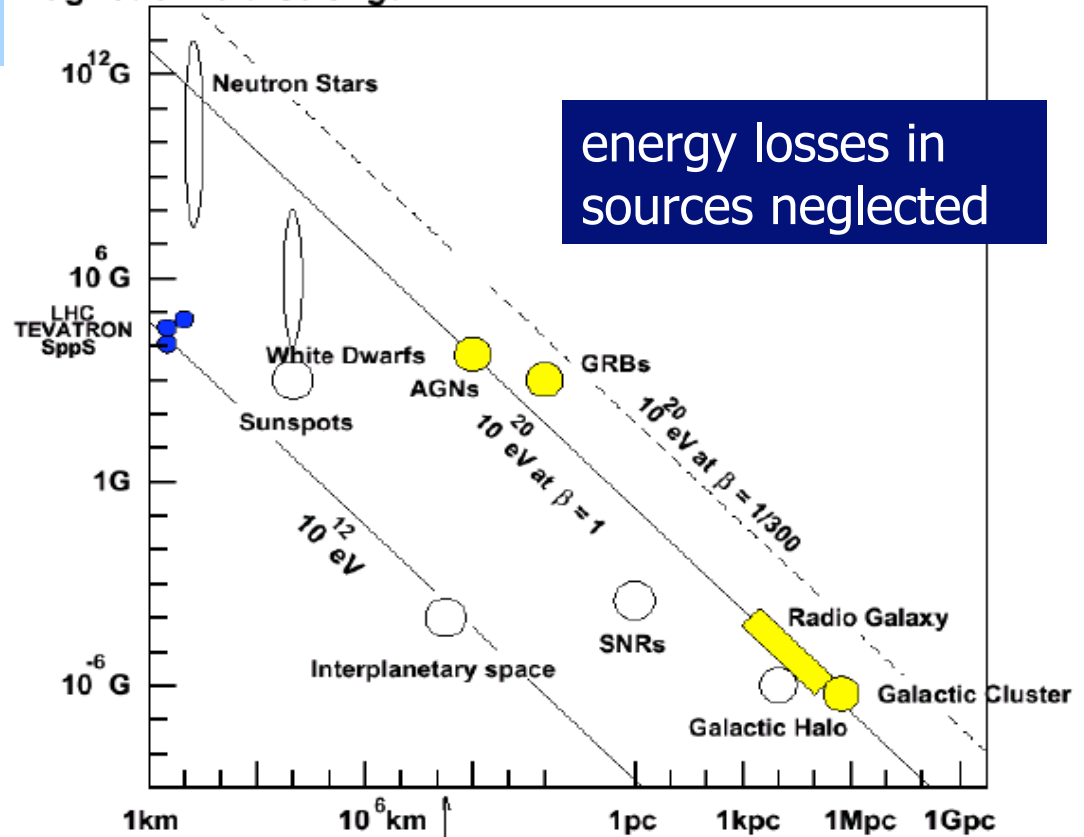
$$\rho_E / \tau_{\text{esc}} \sim 10^{-26} \text{ erg/cm}^3\text{s with galactic escape time}$$

$$\tau_{\text{esc}} \sim 3 \times 10^6 \text{ yrs}$$

SN power: 10^{51} erg/SN + ~ 3 SN per century in disk

$\sim 10^{-25}$ erg/cm³s \Rightarrow 10% of kinetic energy in proton and nuclei acceleration

Magnetic Field Strength



energy losses in sources neglected

R = acceleration site dimensions
The accelerator size must be larger than R_{gyro}

G. Pelletier Fermi acceleration in Lemoine and Sigl

Top-down

Exotic processes

Decays of supermassive particles and topological defects
Z decays due to interactions of UHE neutrinos on relic
Neutrinos

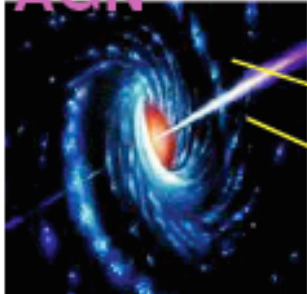
Granted neutrinos:

GZK neutrinos: photopion production on CMWB radiation
Neutrinos from interactions of CRs on ISM

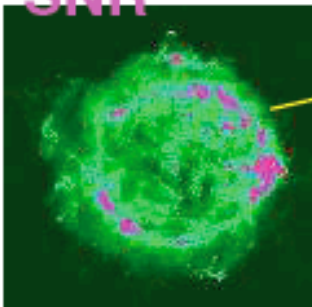
$$E_{\max} \approx \Gamma Z \left(\frac{B}{1\mu G} \right) \left(\frac{R}{1kpc} \right) 10^{18} eV$$

Sources of CRs

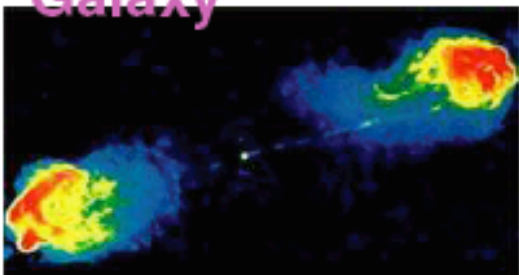
AGN



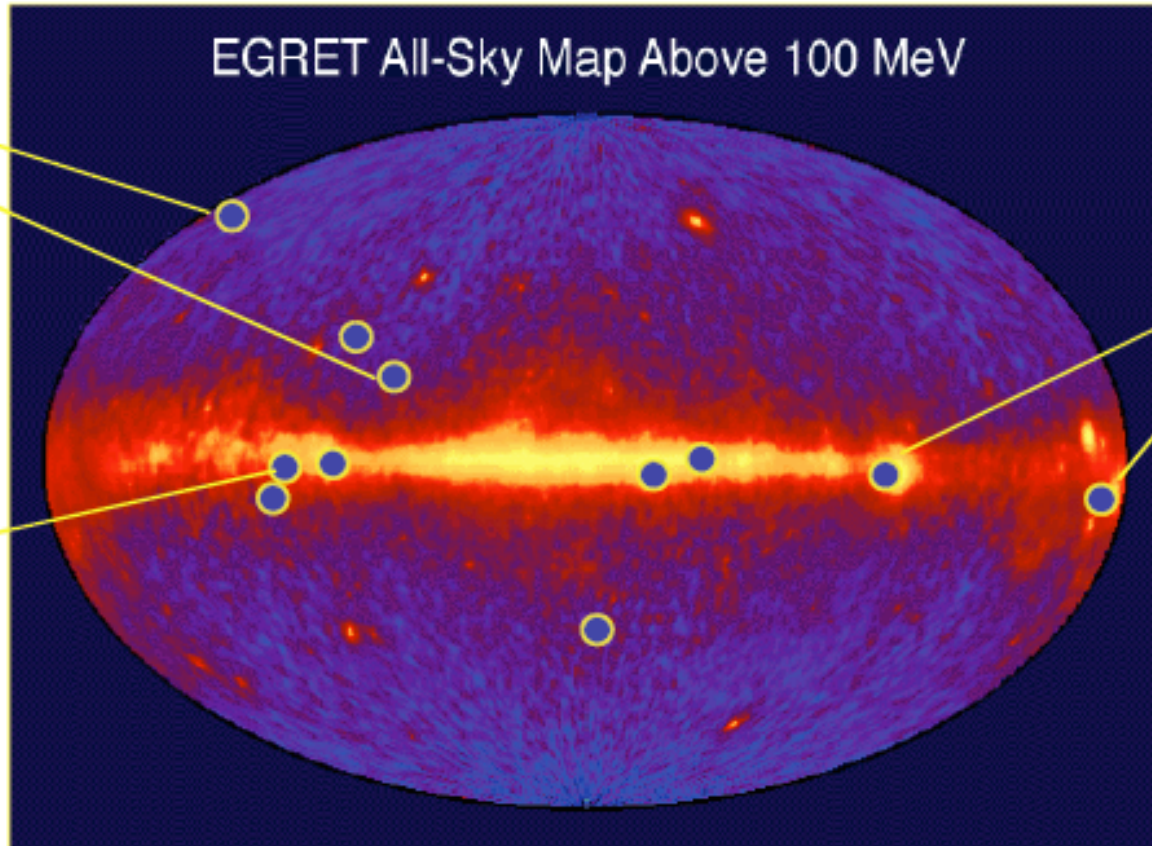
SNR



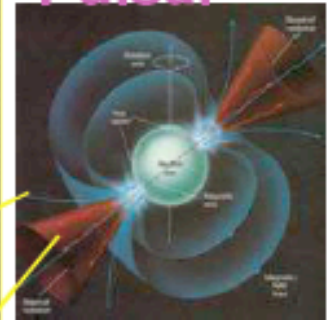
**Radio
Galaxy**



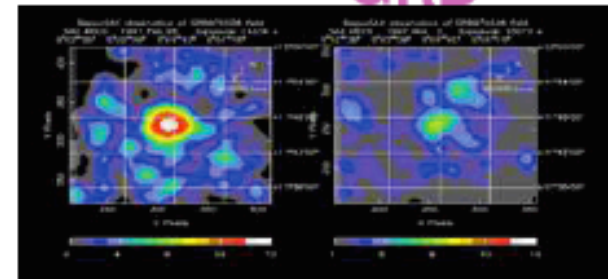
EGRET All-Sky Map Above 100 MeV



Pulsar



GRB



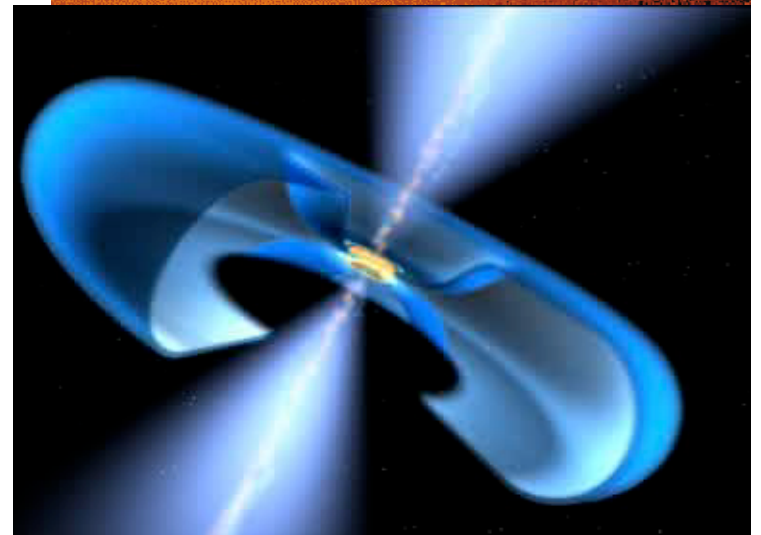
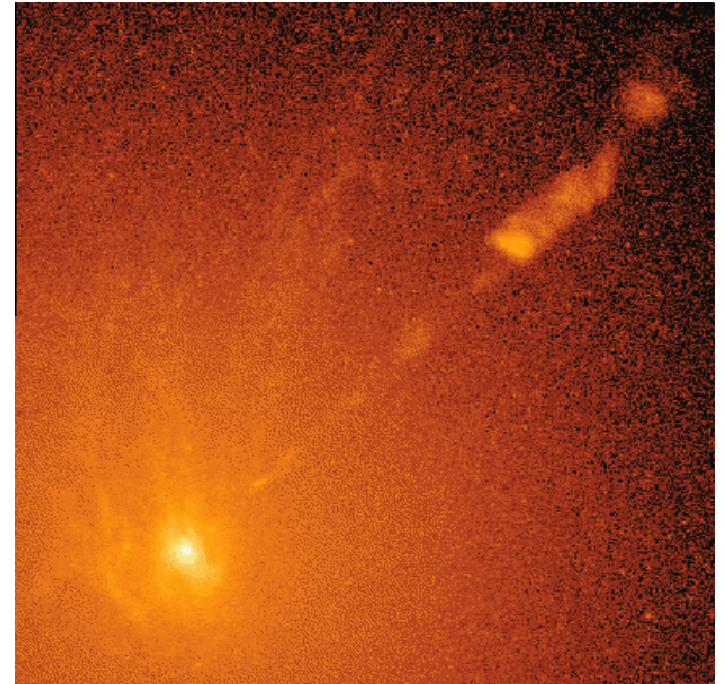
The most powerful accelerators

- AGNs are good candidates because the accretion flow towards a central black hole concentrates magnetic field over a large volume. $B \sim$ few kG in the vicinity of a $10^8 M_{\text{sun}}$ on scales of few astronomical units. Some AGNs have large jets of several hundred kpc length revealed by their synchrotron radiation. When the jet is towards us they are called blazars.

- GRB: Prof Waxman

Very attractive accelerator since Lorentz factors of the relativistic flow can be large

$\Gamma = 100-1000$



Observed AGN spectra

Average SED=spectral energy distribution of blazars

2 broad peaks: the first located in the IR-soft X-ray band is due to synchrotron

Emission, while the second to IC

By the same electrons producing

the synchrotron part of the

spectrum. The 0.1-10 keV

emission of blazars is located at

the minimum between the 2.

Exception to these are flaring AGNs

Which show a synchrotron peaking

above 10 keV (Mrk 501 peak

Shifted at 100 keV in the Apr 97

Flare)

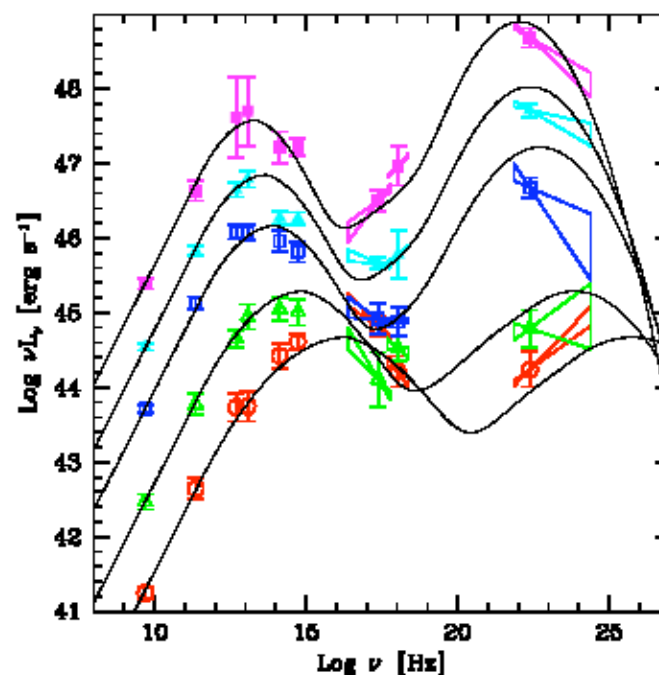


Fig. 10. The average SED of the blazars studied by Fosati et al. (1998), including the average values of the hard X-ray spectra. The thin solid lines are the spectra constructed following the parameterization proposed in this paper.

Gamma-Ray Bursts

Vela-4 detects the 1st γ emission $E_\gamma > 0.1$ MeV on July 2nd, 1967

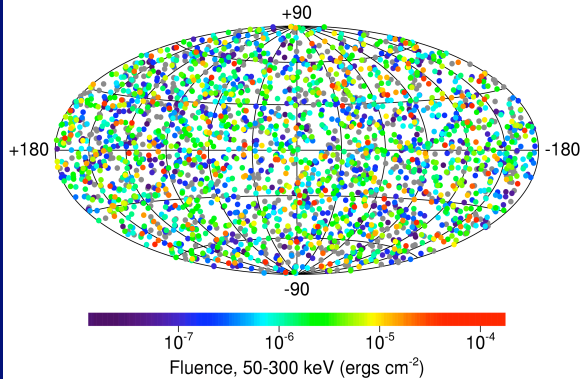
BATSE (~1 GRB/d, 3° error box, FoV 4π sr)

EGRET (1 GRB/yr, 10 arcmin, $E > 30$ MeV, FoV 0.6 sr)

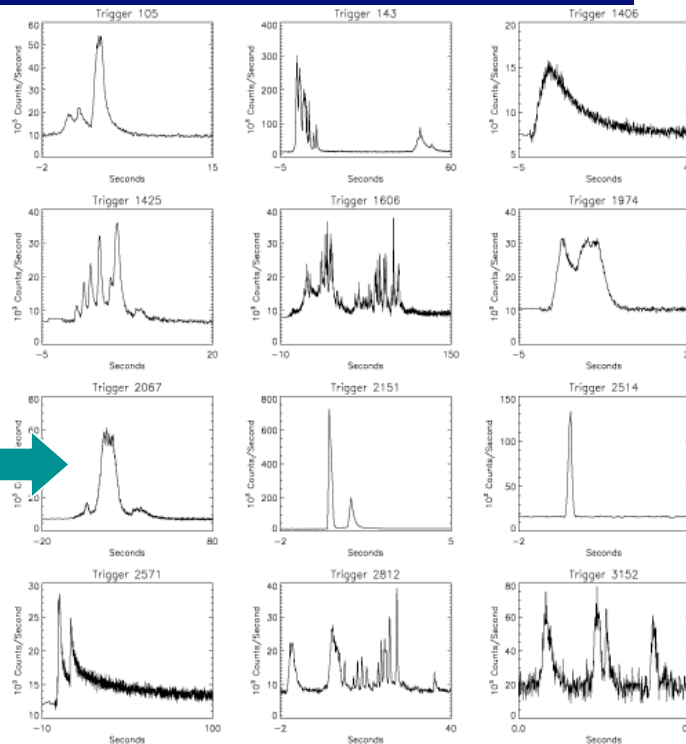
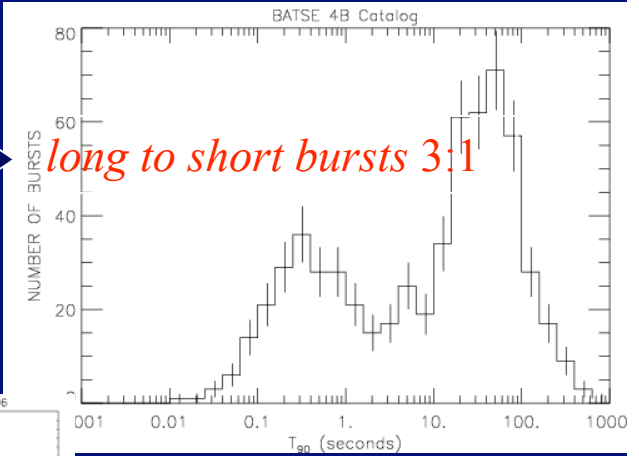
Bimodal duration distribution

Isotropic Angular Distribution

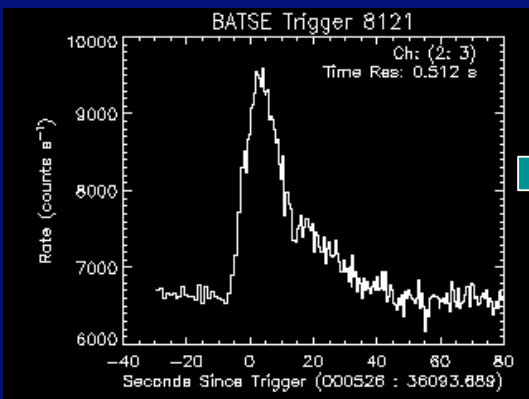
2704 BATSE Gamma-Ray Bursts



1 arcmin = 1/60 deg



Counting rates with time variable from GRB to GRB



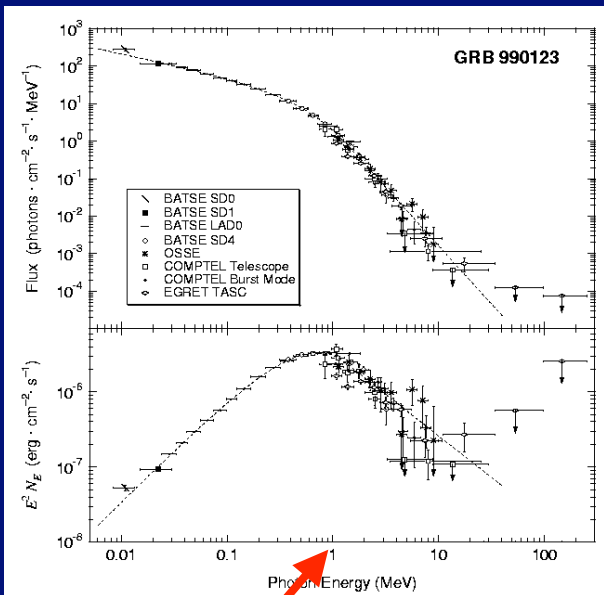
BATSE observations on GRBs



Spectra

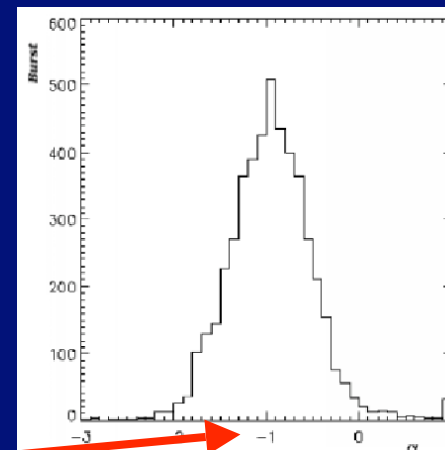
GRBs

$$N_E(E) \propto \begin{cases} E^\alpha e^{-\frac{E}{E_0}}, & E \leq E_0 \\ E^\beta, & E > E_0 \end{cases}$$



Band et al.

Parametri:
 α, β e E_0

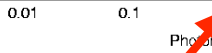
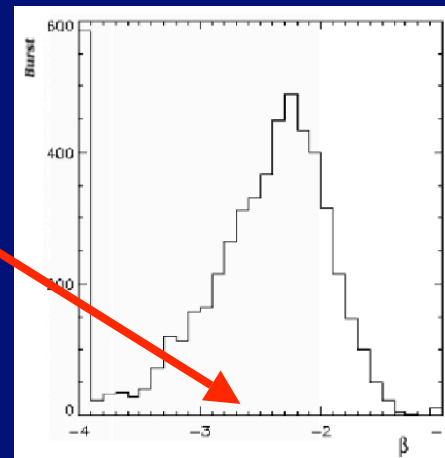
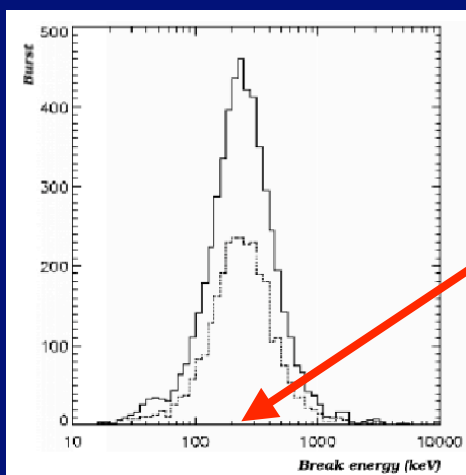


$\alpha \sim -1$

$\beta \sim -2$

$E_0 \sim 200 \text{ keV}$

E_0



Beppo-SAX and afterglows

Beppo-SAX (54 GRBs/6yrs, 5' error box, 40-700 keV, FoV 20 ° × 20 °)

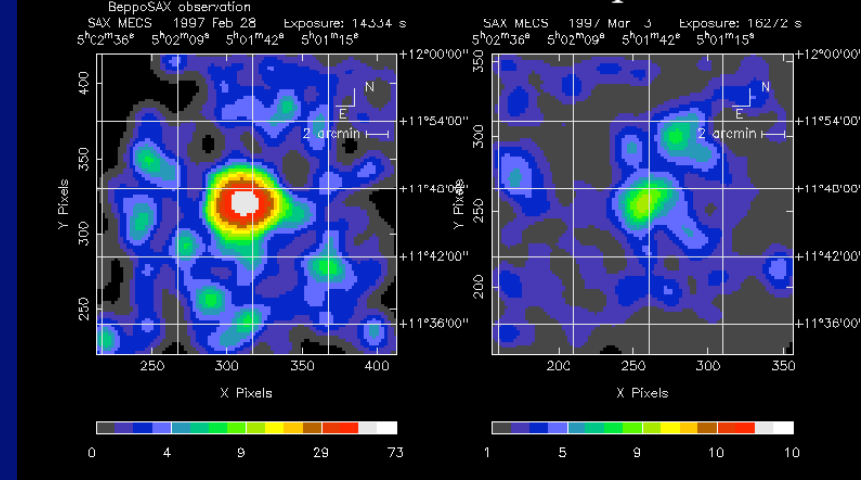
Determined in 5-8 h precise GRB position thanks to detection in X (WFC)

Xray afterglow discovery: delayed emission even after ~ 1d ⇒ optical counterparts

SN association: GRB980425-SN1998bw
GRB030329-SN2003dh position coincidence and SN like spectrum in afterglow

Long GRBs: stellar core collapse into a BH, accretes mass driving a relativistic jet that penetrates the mantle and produces GRB

Costa, E. et al., astro-ph/9706065



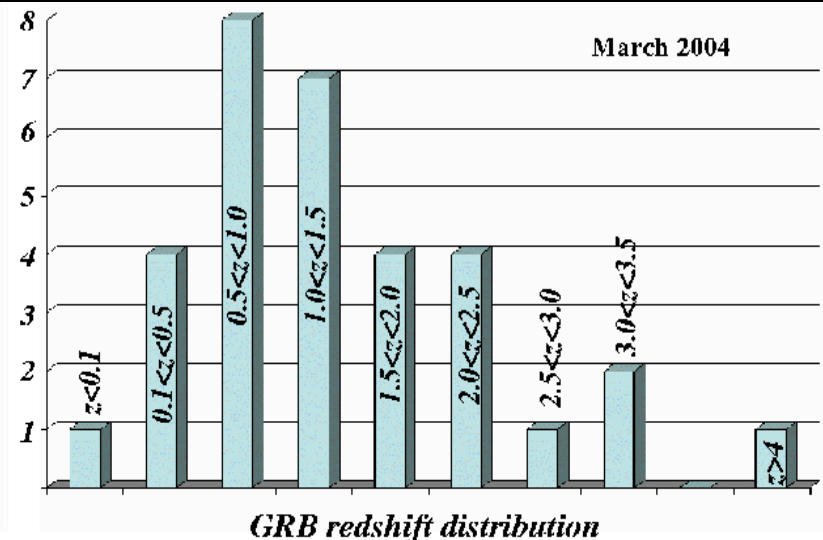
From optical afterglow spectrum redshift ⇒ cosmological distance

Emitted energy (isotropic) $\sim 10^{54}$ erg

Beaming (light curve changes in slope):

$$\theta = 1/\Gamma E_{\text{obs}} = \Gamma E_{\text{emitted}} \quad \Gamma \sim 10^2 - 10^3$$

$$E_{\text{emitted}} \sim 5 \cdot 10^{50} \text{ erg}$$

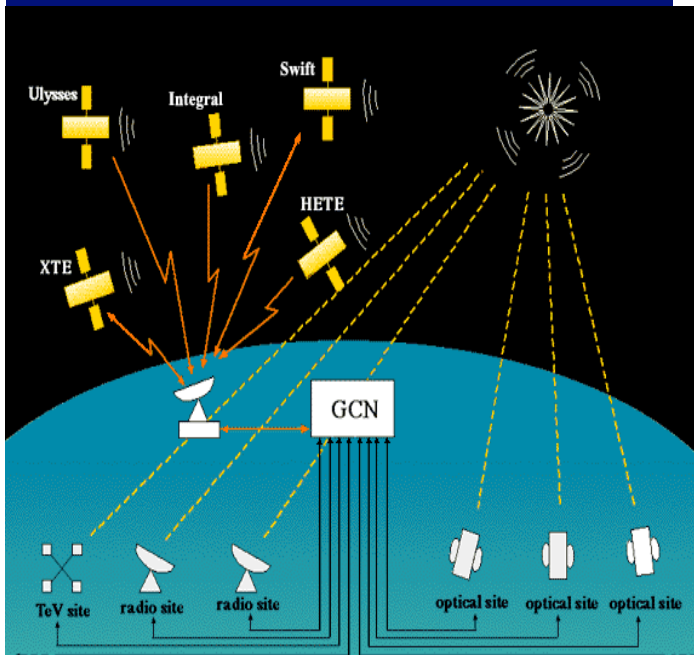


Current and future missions

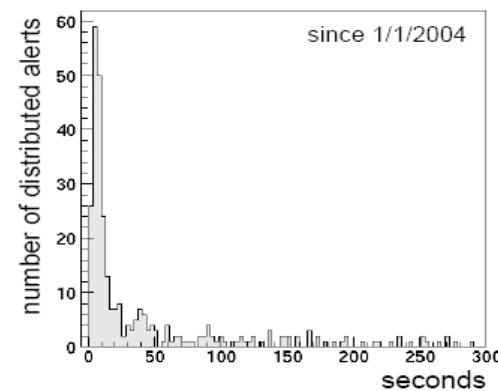
Mission	Error box (°)	Rate (GRB/yr)
GLAST	<0.125	300
SWIFT	~0.004	200
HETE-2	~0.03	25
INTEGRAL	<0.2	35

Delay of satellite data processing and transmission+transmission of alerts

The Gamma-ray bursts Coordinate network GCN: Distribution of alerts

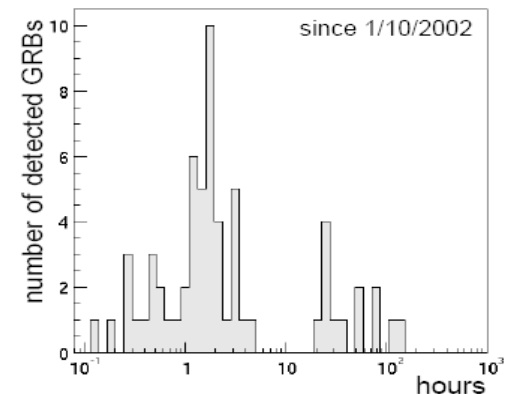


Time between the detection of the gamma rays and the arrival of the alert message at the site



1-2 alert messages per day

Time between the alert message and the final message



~30 GRBs per year

The fireball model

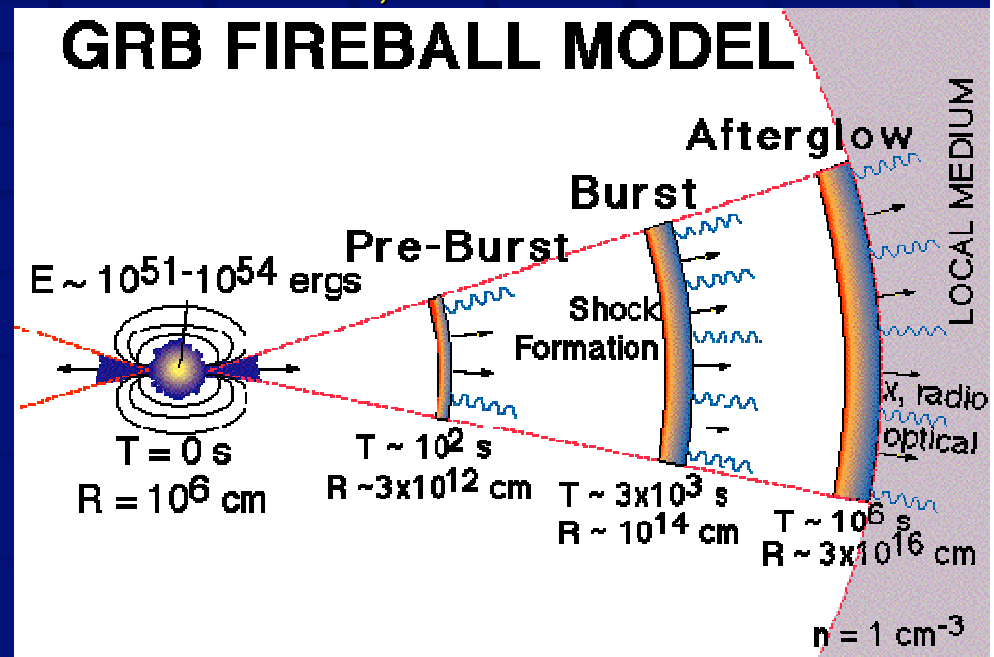
Compactness problem: the optical depth for pair production very high if initial energy emitted from a volume with radius $R < c dt \sim 300 \text{ km}$ with $dt =$ variability time scale $\sim \text{ms}$ in photons with the observed spectrum \Rightarrow this would imply thermal spectra contrary to observations

Solution: relativistic motion dimension of source $R < \Gamma^2 c dt$ and $E_{\text{obs}} = \Gamma E_{\text{mitted}}$

A fireball (γ , e^\pm , baryon loading $< 10^{-5} M_{\text{sun}}$ to reach observed Γ) forms due to the high energy density, that expands. When it becomes optically thin it emits the observed radiation through the dissipation of particle kinetic energy into relativistic shocks

External shocks: relativistic matter runs on external medium, interstellar or wind earlier emitted by the progenitor

Internal shocks: inner engine emits many shells with different Lorentz factors colliding into one another, and thermalizing a fraction of their kinetic energy



Review <http://arxiv.org/pdf/astro-ph/0405503>

Energy spectrum for various components at low energies

Below 1 GeV/nucleon there is a pronounced attenuation for all species varying with the phase of the solar cycle (flux is minimum when solar activity is maximum)

Cut-off due to propagation in magnetic field carried by solar wind (solar modulation)

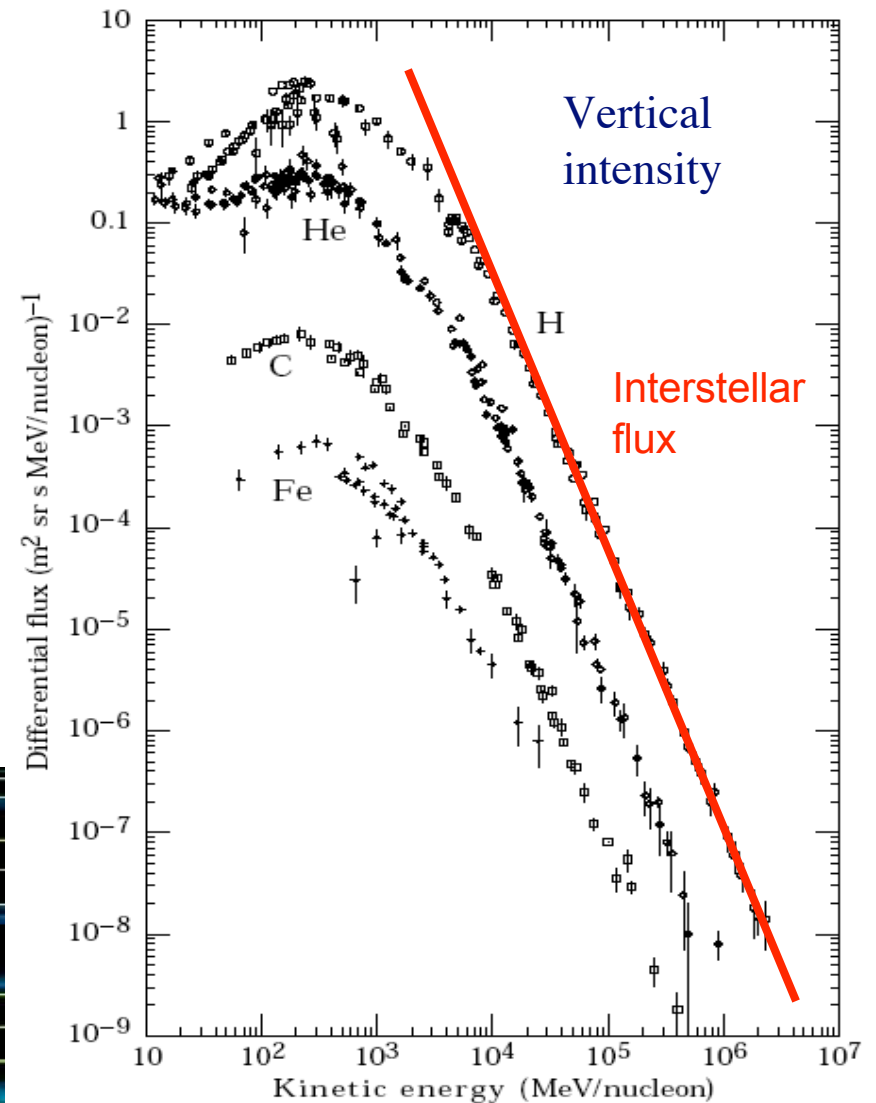
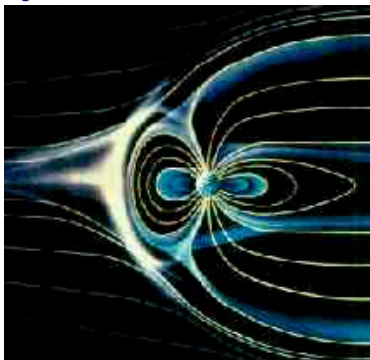
The solar wind is the outflow of material from the surface of the Sun (solar corona) traveling at ~ 450 km/s. The magnetic field ($\sim 5 \cdot 10^{-5}$ G) is frozen in the ionized material and is dragged outwards from the Sun. The effect influences different elements with same velocity in the

same way since $\propto Fe$

$A/Z \sim 2$

and the rigidity is

$R = (A/Z)(m_p \gamma v c / e)$

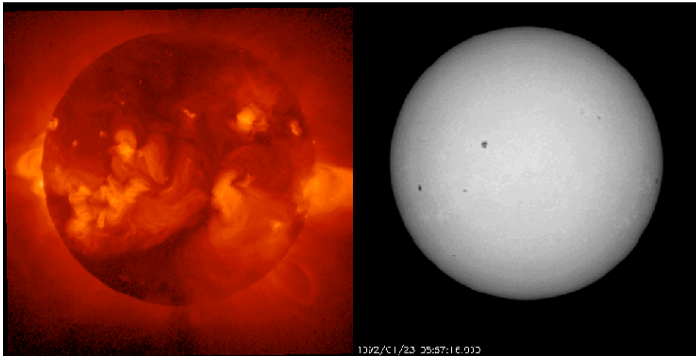


Low energy spectrum: Solar modulation

Neutron monitors: ground based detectors that count secondary CRs that reach the observation level (eg. neutrons from evaporation of nuclei by CRs) 11 yrs cycle

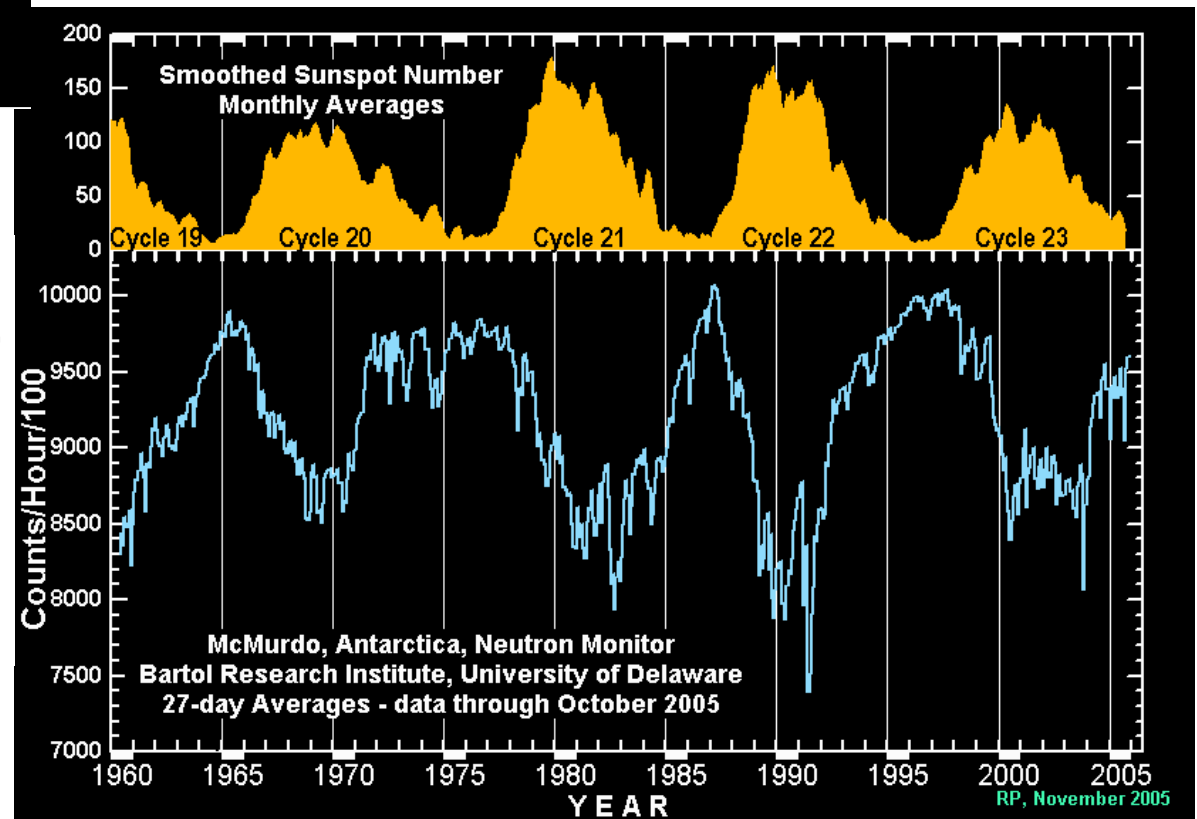
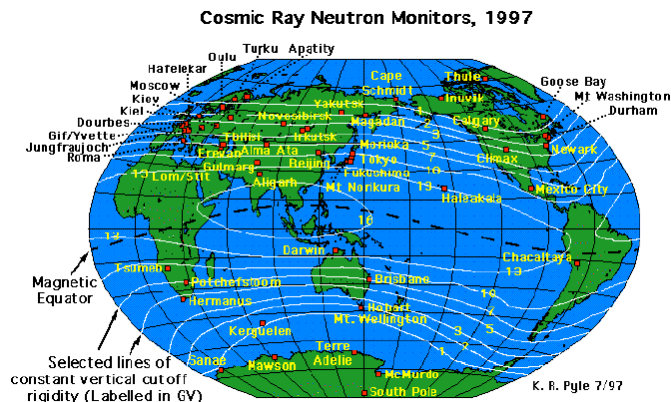
X-rays

Visible light

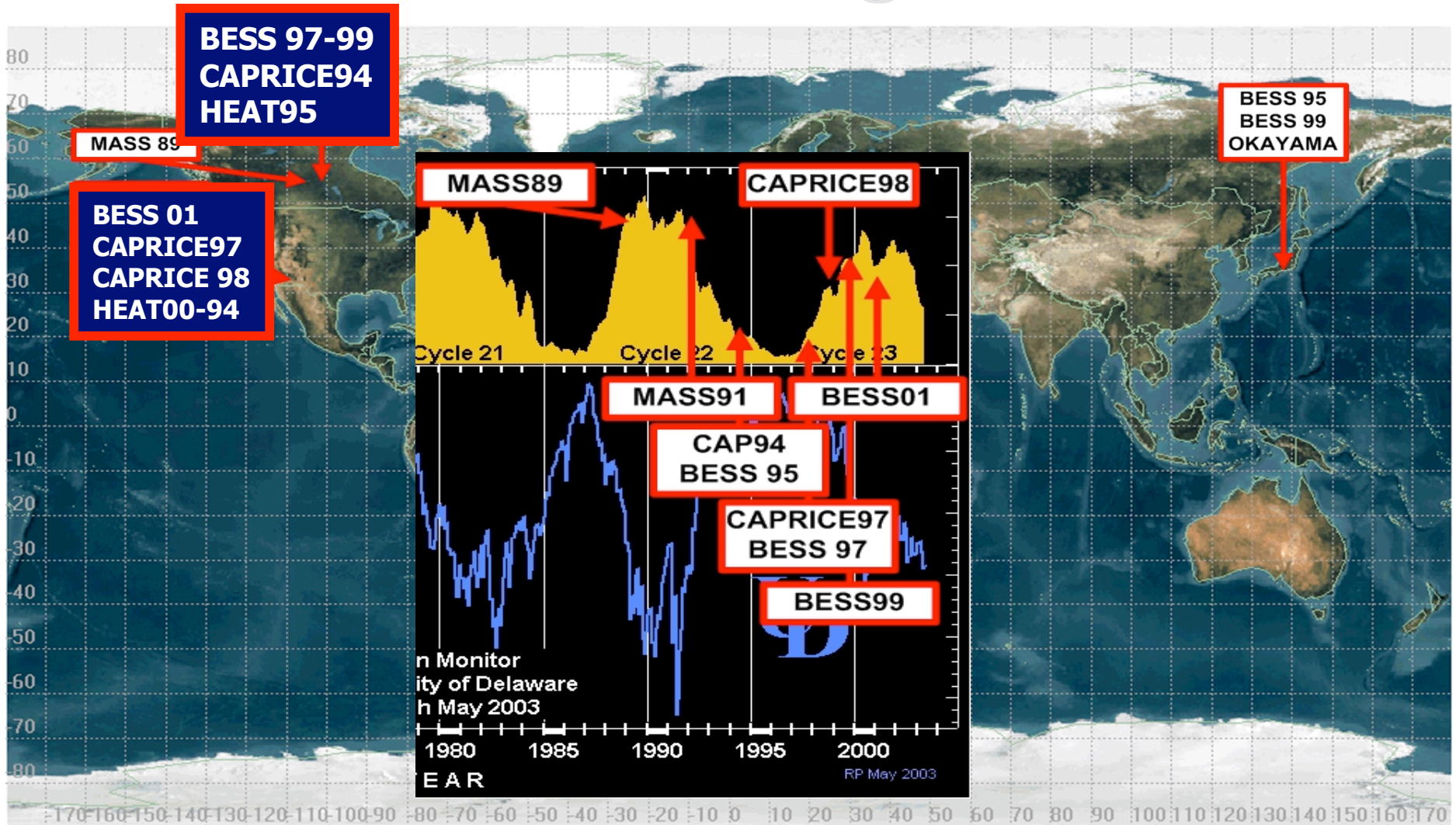


<http://neutronm.bartol.udel.edu/>

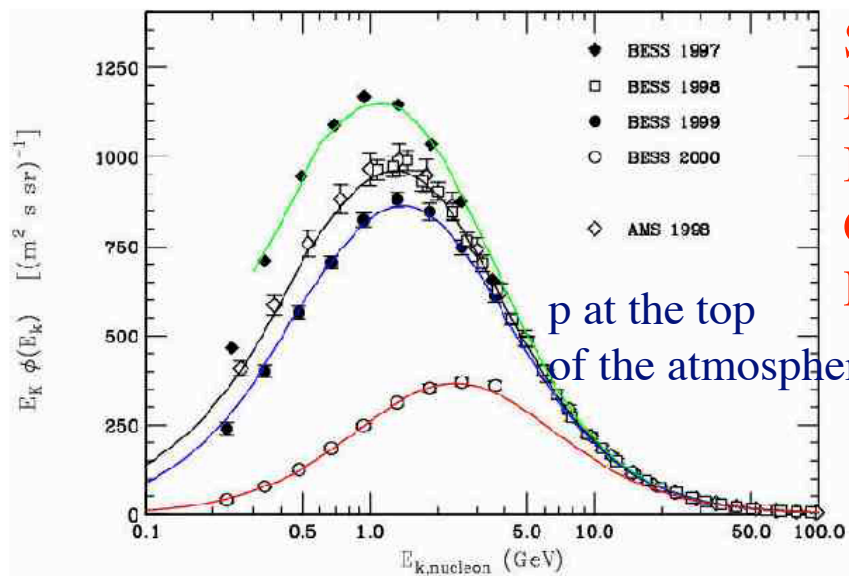
Sun spots are indication of Sun activity



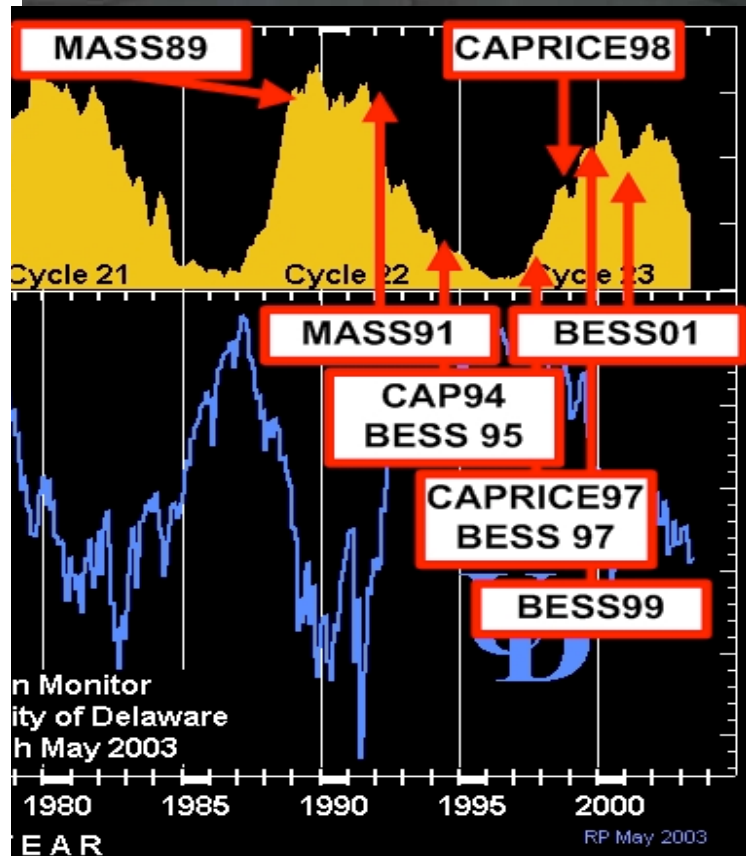
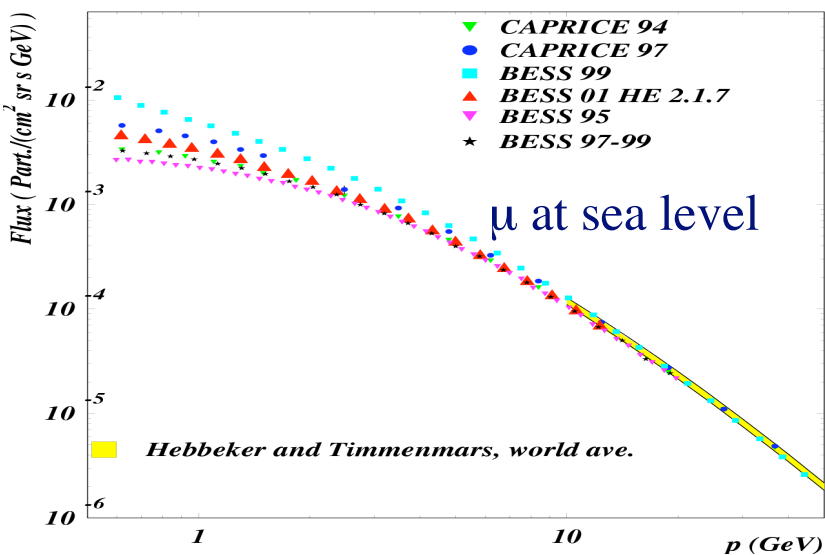
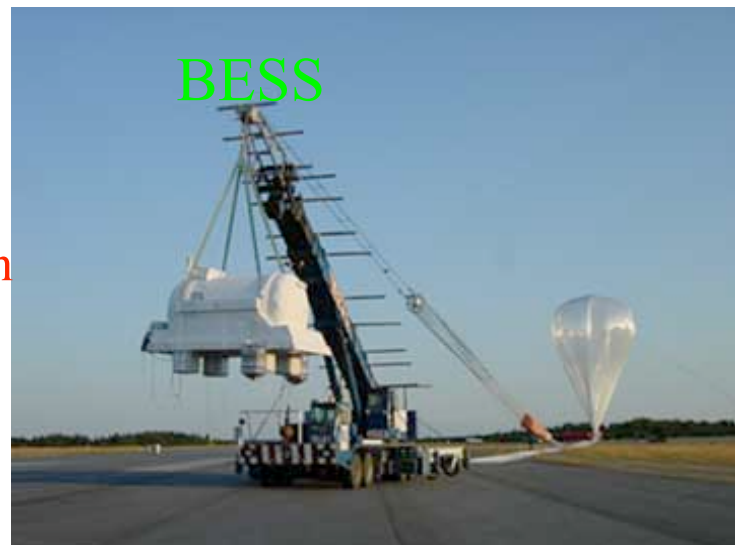
Balloon flights



Ballon flight muon flux and Solar modulation

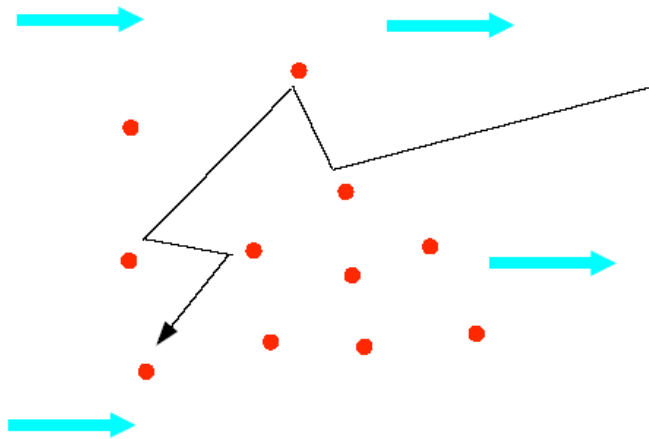


Same location
 MASS 89
 BESS 97-99
 Caprice 94
 Heat 95



Formalism of solar modulation: time variations in the CR spectrum

Moving magnetic scattering centers



Propagation of charged particle in a plasma

The solar modulation parameter is given by

$$\phi = \frac{1}{3} \int_{r_1}^{r_2} \frac{v}{K} dr$$

$$K \propto \beta R$$

Where the diffusion coefficient is

And r_1 = heliospheric radius of the Earth (1AU) and r_2 is the boundary of the heliosphere 50 AU

1AU =149 598 000 kilometers

The effect of solar modulation is equivalent to a potential with particles losing an energy $\Delta E = |Z|\phi$. A particle with total energy E_{IS} in the interstellar space would reach the Earth with energy E : $E = E_{IS} - |Z|\phi$

The flux of particles at Earth is related to the interstellar one by (m =particle mass)

$$\Phi(E) = \frac{(E^2 - m^2)}{(E_{IS}^2 - m^2)} \times \Phi_{IS}(E_{IS})$$

Geomagnetic effects

The magnetic field prevents low rigidity particles from reaching the surface of the Earth.

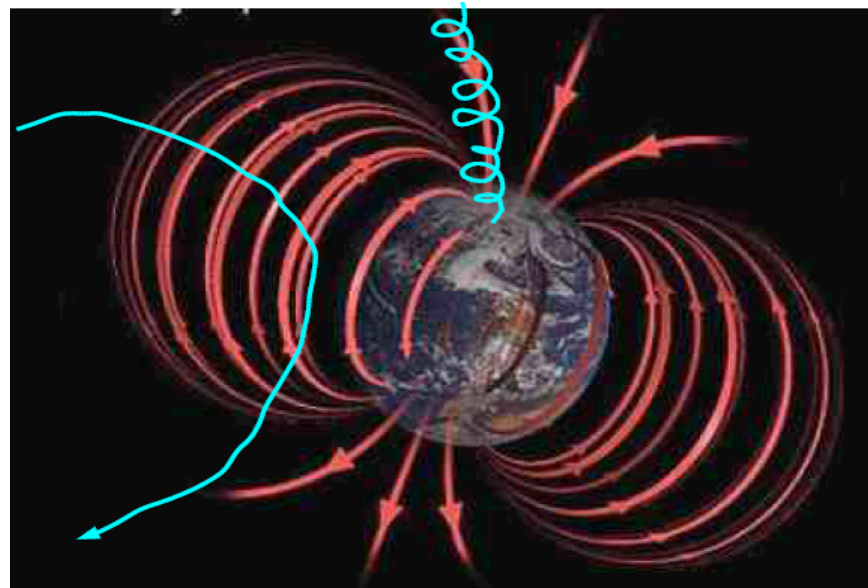
The isotropy of the CR flux is spoiled by the Earth magnetic field

The effect depends on the rigidity (momentum/charge) and direction of the particle and latitude of the detector

$$\phi_{\vec{x}}(p, \Omega) = \phi_{\infty}(p) \times \zeta(p, \Omega, \vec{x})$$

ζ is either 0 or 1
Penetration probability

Flux at many radii from the Earth corrected for solar modulation



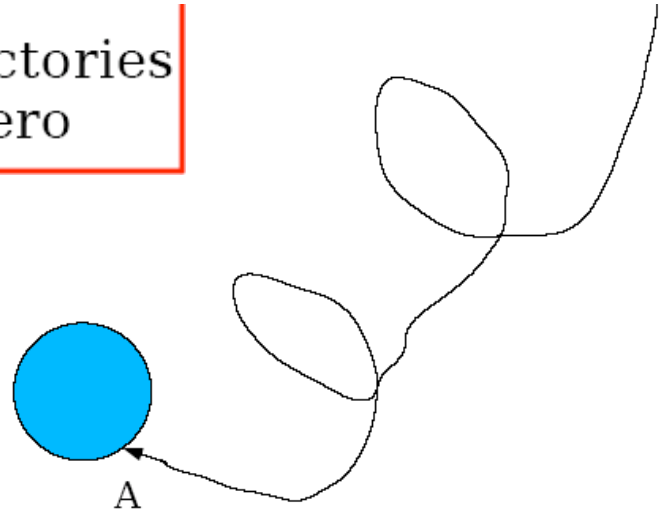
Latitude Effect

At the magnetic pole particles of any rigidity can arrive

Forbidden Trajectories

For forbidden trajectories
the flux must be zero

A trajectory is forbidden if $\lambda =$ latitude of detector, Ω and R are such that the particle should have been originated from the Earth or it remains confined close to the Earth

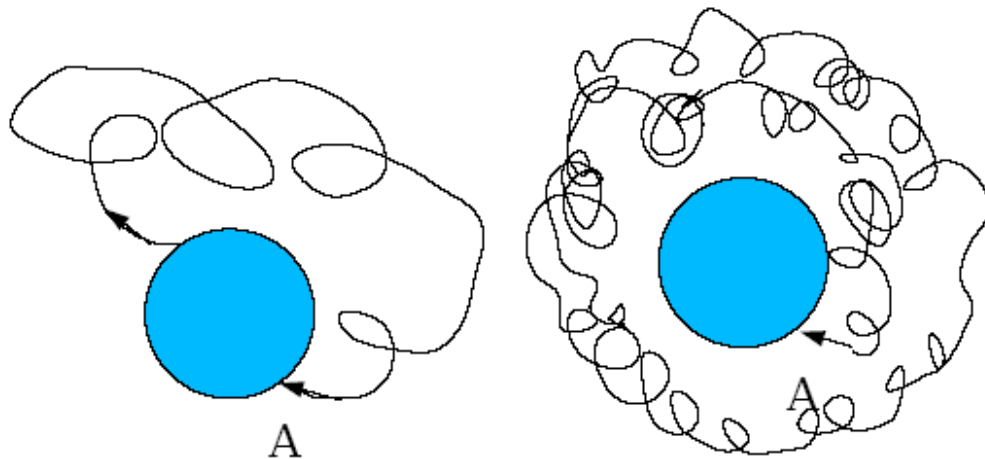


An allowed trajectory extends to infinity

Stoermer: solved analytically the equation motion in a dipole field.

For particles that penetrate vertically towards the center of the magnetic dipole the minimum rigidity to penetrate the distance r from the center of the magnetic dipole is

$$R_s \geq 59.4GV \left(\frac{r_{\oplus}}{r} \right) \cos^4 \lambda_B / 4$$



$M/2r_{\oplus}^2 = 59.4$ GV is the rigidity of a particle in a circular orbit of radius r_{\oplus} in the equatorial plane of the dipole field

The Stoermer formula and the East-West effect

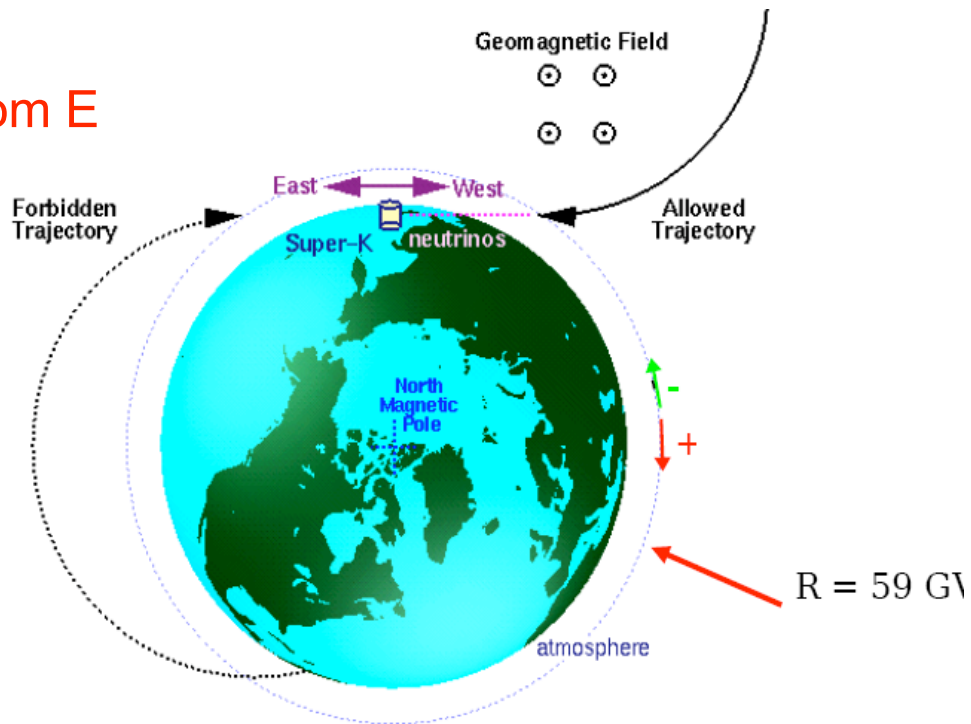
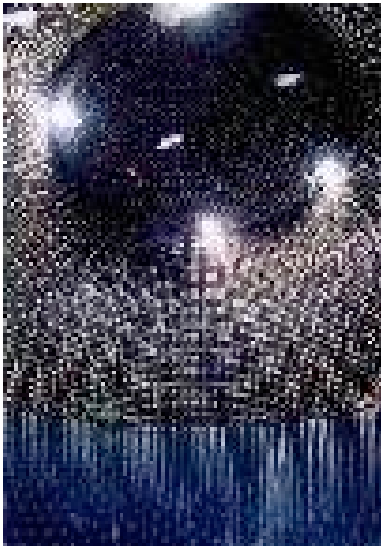
In general for a particle with zenith angle θ and azimuth φ measured clock-wise from the direction of the magnetic S

$$R_S(r, \lambda_B, \vartheta, \varphi) = \left(\frac{M}{2r^2} \right) \left[\frac{\cos^4 \lambda_B}{[1 + (1 - \cos^3 \lambda_B \sin \vartheta \sin \varphi)^{1/2}]^2} \right]$$

φ = azimuth measured clock-wise from magnetic S direction

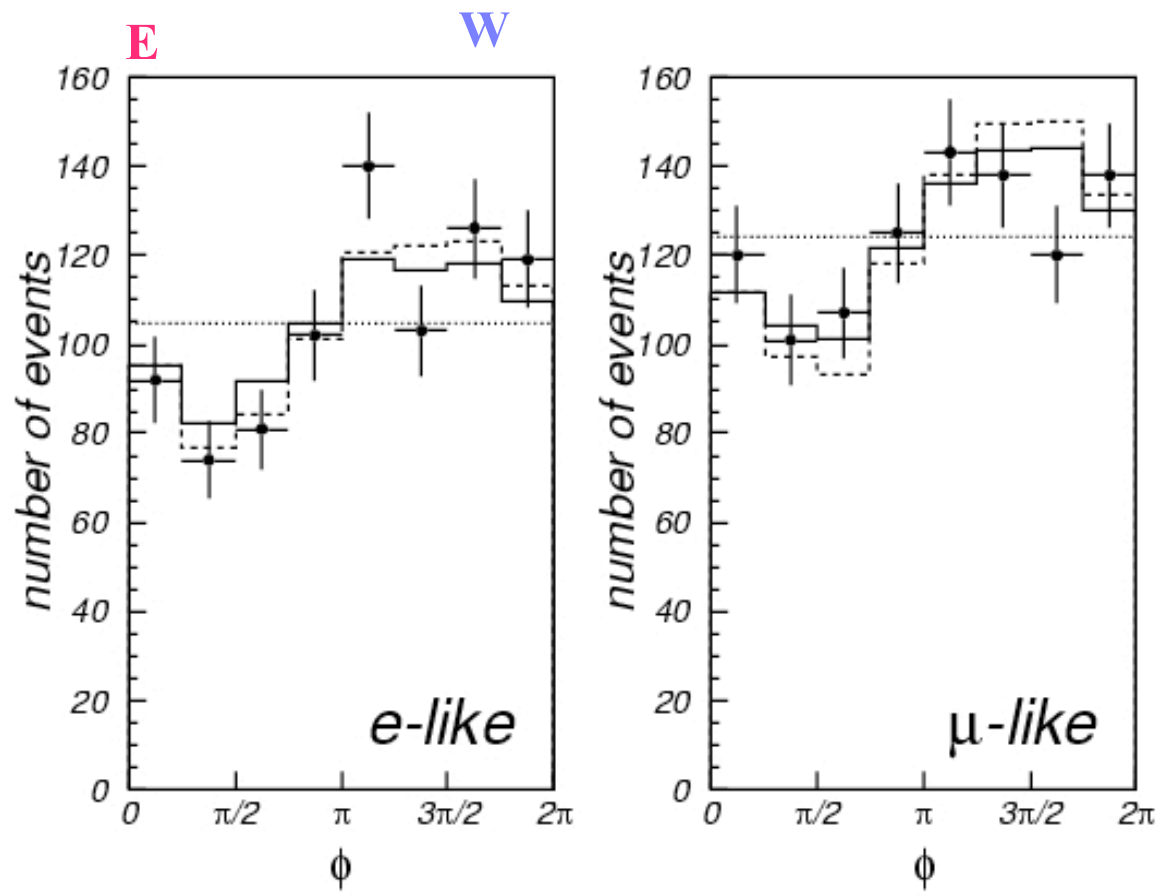
Given the dependence on $\varphi \Rightarrow$ E-W effect: for positively charged particles with the same zenith angle the cut-off is higher from E than W and viceversa for negative charges

CRs are almost all positive
deficit of particles arriving fom E

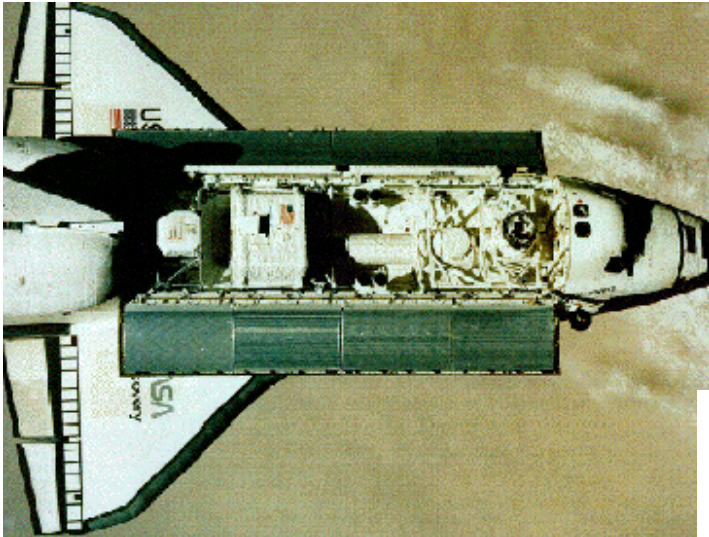


East-West effect in neutrinos

Super-Kamiokande East-West asymmetry in azimuth

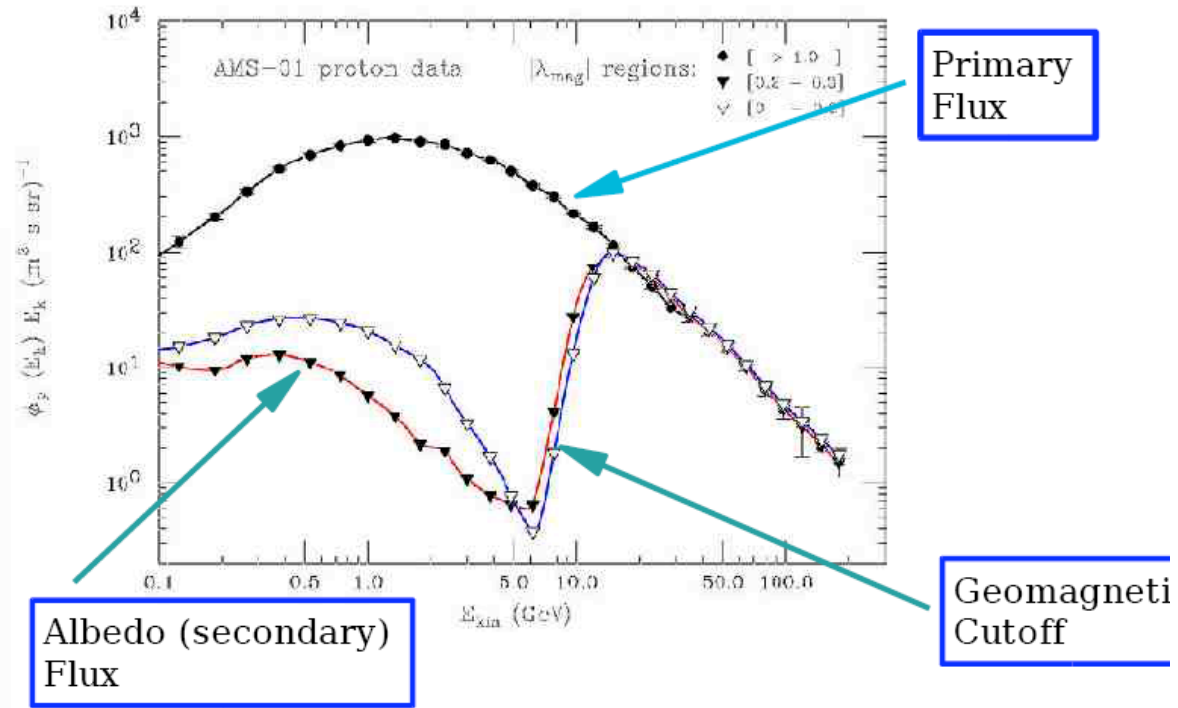
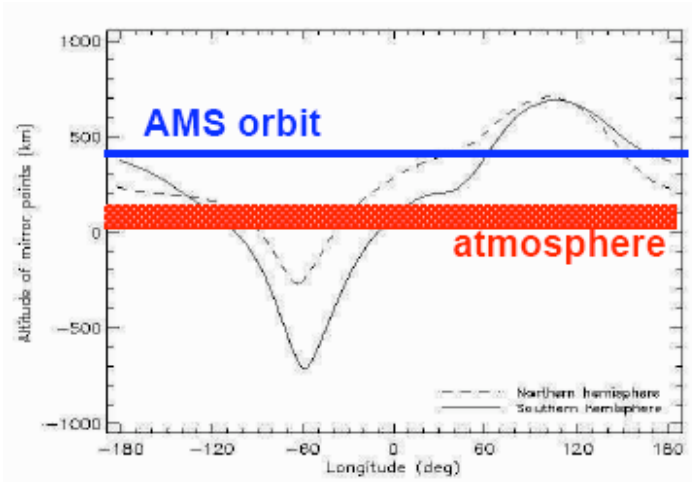


AMS-01 measurement of albedo



Proton Measurements

$$\lambda_{\text{mag}} < 0.2 \text{ (} 11.5^\circ \text{)}$$



Other components: electrons and anti-p

Electrons are believed to be primary particles + secondaries produced in propagation; positrons are generated in the propagation in the Galaxy. There is the interesting possibility of a primary component of positrons generated by DM particles in e^+e^- decays. The corresponding spectrum should peak at $1/2 m_{\text{DM}}$.

Electrons and positrons lose energy through synchrotron radiation in magnetic fields and bremsstrahlung in the ISM and in IC scatterings on radiation fields.

The electron+positron spectrum is steeper than proton/nuclei one at the top of the atmosphere.

$e^+/e^- \sim 0.2 < 1$ GeV

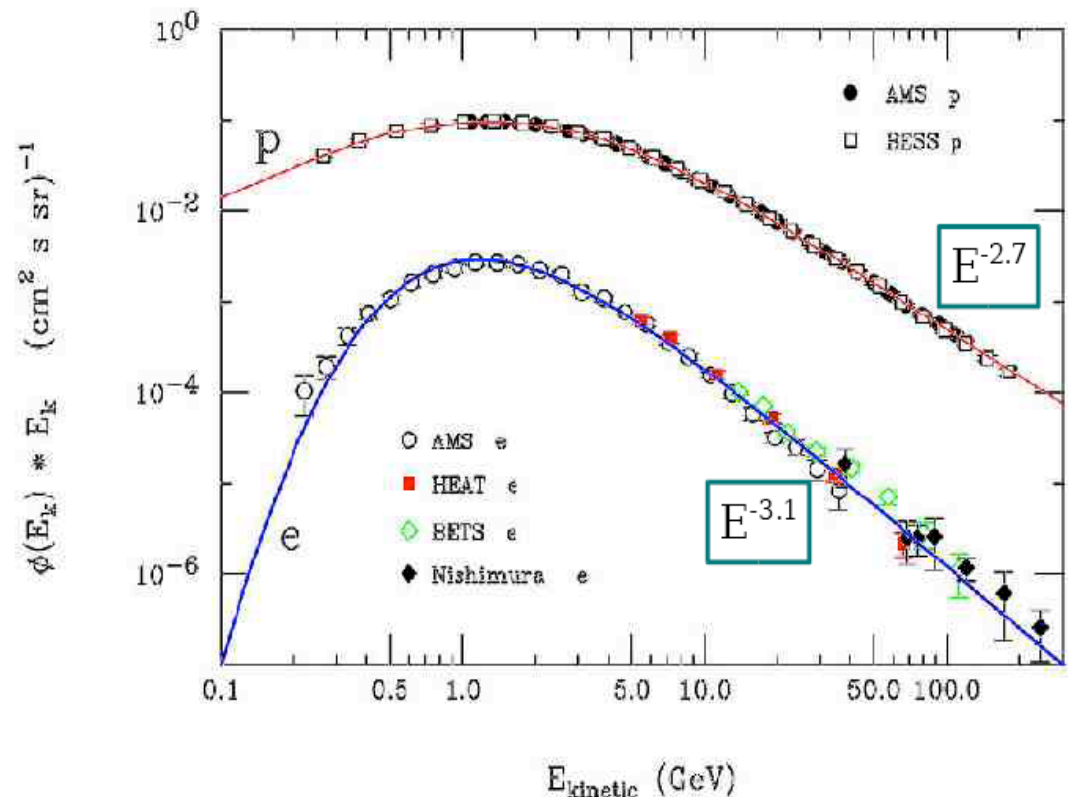
and 0.05 between

5-20 GeV consistent with secondary origin

Anti-p/p $\sim 2 \cdot 10^{-4}$ at around 10-20 GeV.

Unless there is an antimatter section of the Galaxy, anti-p are secondaries. The absolute threshold $7 m_p \sim 7$ GeV for $pp \rightarrow ppp\bar{p}$

And the secondary spectrum peaks at 2 GeV



Cosmic rays in the atmosphere

The atmosphere contains about 25 radiation lengths and 11 interaction lengths

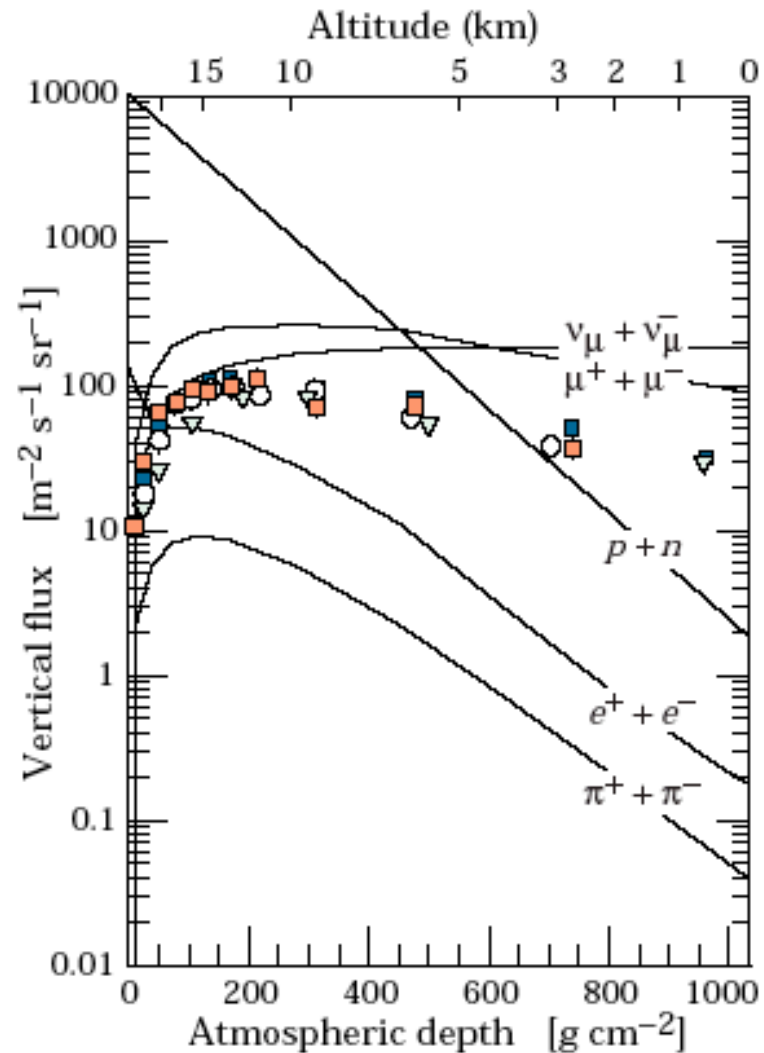


Figure 24.3: Vertical fluxes of cosmic rays in the atmosphere with $E > 1$ GeV estimated from the nucleon flux of Eq. (24.2). The points show measurements of negative muons with $E_\mu > 1$ GeV [4,19,20,21].

Some useful quantities

$$\sigma_{p \text{ Air}}(E) \simeq 300 \text{ mbarn}$$

$$\lambda_{\text{int}}(E) = \frac{AM_N}{\sigma_{\text{int}}(E)} \simeq 80 \text{ g cm}^{-2}$$

$$X \sim \lambda_{\text{int}} \sim 80 \text{ g cm}^{-2}$$

$$X_{\text{atm}} \simeq 1033 \text{ g cm}^{-2}$$

$$\langle h \rangle \sim \frac{18 \text{ Km}}{\cos \theta_{\text{zenith}}}$$

Suggested readings

- Cosmic Rays

Longair Vol 1 High Energy Astrophysics

Stanev High Energy Cosmic rays

M. Lemoine & G. Sigl, Physics and Astrophysics of Ultra-High-Energy Cosmic Rays

<http://pdg.lbl.gov/2005/reviews/cosmicrayrpp.pdf>

<http://arxiv.org/pdf/astro-ph/0511235>

Horandel [astro-ph/0501251](http://arxiv.org/pdf/astro-ph/0501251)